

Original Article

Overexpression of miR-506 inhibits growth of osteosarcoma through Snail2

Zhongxiang Yu^{1*}, Yuting Zhang^{2*}, Ningyang Gao¹, Xiang Wang¹

¹Department of Orthopaedics, Shu Guang Hospital Affiliated to Shanghai Traditional Chinese Medical University, Shanghai 201203, China; ²Department of Orthopaedics and Trauma, Shanghai Putuo District Central Hospital Affiliated to Shanghai Traditional Chinese Medical University, Shanghai, 200062, China. *Equal contributors.

Received October 12, 2015; Accepted November 18, 2015; Epub December 15, 2015; Published December 30, 2015

Abstract: Osteosarcoma (OS) is a prevalent primary bone malignancy and its distal metastasis accounts for the majority of OS-related death. MicroRNAs (miRNAs) play critical roles during cancer metastasis. Thus, elucidation of the involvement of specific miRNAs in the metastasis of OS may provide novel therapeutic targets for OS treatment. Here, we showed that in the OS specimens from patients, the levels of miR-506 were significantly decreased and the levels of Snail2 were significantly increased, compared to the paired normal bone tissue. MiR-506 and Snail2 inversely correlated in patients' specimen. Bioinformatics analyses predicted that miR-506 may target the 3'-UTR of Snail2 mRNA to inhibit its translation, which was confirmed by luciferase-reporter assay. Moreover, miR-506 overexpression inhibited Snail2-mediated cell invasiveness, while miR-506 depletion increased Snail2-mediated cell invasiveness in OS cells. Together, our data suggest that miR-506 suppression in OS cells may promote Snail2-mediated cancer metastasis.

Keywords: Osteosarcoma (OS), Snail2, miR-506

Introduction

Osteosarcoma (OS) is a prevalent primary bone malignancy [1-6]. The combined chemotherapy and surgery have been applied as a regular therapy for OS, which has increased the 5-year survival of patients minimally, largely due to the distal metastasis of OS cells [1-6]. Therefore, approaches to suppress the invasion and metastasis of OS appear to be critical for effective treatments. A number of human OS cell lines have been established, among which U2OS [7] cell line has been extensively characterized and widely used in research.

Zinc finger protein Snail2 belongs to the Snail family of C2H2-type zinc finger transcription factors, and is encoded by the SNAI2 gene in human [8, 9]. Snail2 acts as a transcriptional repressor that binds to E-box motifs to repress E-cadherin transcription in some cancer cells. Thus, Snail2 is potent trigger for epithelial-mesenchymal transition (EMT) to allow cancer cells to invade and migrate [10-14].

MicroRNA (miRNA) is a class of non-coding small RNA of comprised of about 18-23 nucleotides. MiRNAs regulate the gene expression post-transcriptionally, through its base-pairing with the 3'-untranslated region (3'-UTR) of the mRNA of the target gene [15, 16]. It is well-known that miRNAs regulate various biological events including carcinogenesis [17-19]. Among all miRNAs, miR-506 is relatively less studied. Recently, a role of miR-506 as a tumor suppressor has been acknowledged in some types of cancers [20-27]. However, its participation in the metastasis of OS has not been appreciated.

In this study, we found that in OS, miR-506 levels were significantly decreased and Snail2 levels were significantly increased, compared to paired normal bone tissue. MiR-506 and Snail2 inversely correlated in patients' specimen. Bioinformatics analyses predicted that miR-506 targeted the 3'-UTR of Snail2 mRNA to inhibit its translation, which was confirmed by luciferase-reporter assay. MiR-506 overexpres-

MiR-506 inhibits Snail2-mediated metastasis of OS

sion inhibited Snail2 and cell invasiveness, while miR-506 depletion increased Snail2 and cell invasiveness.

Materials and methods

Patient tissue specimens

A total of 36 resected specimens from OS patients were collected for this study. OS specimens were compared with the paired normal bone tissue (NT) from the same patient. All specimens had been histologically and clinically diagnosed at the Department of Orthopaedics, Shu Guang Hospital affiliated to Shanghai Traditional Chinese medical University from 2007 to 2014. For the use of these clinical materials for research purposes, prior patient's consents and approval from the Institutional Research Ethics Committee were obtained.

Culture of human OS cell line

U2OS is a widely used human OS line purchased from American Type Culture Collection (ATCC, Rockville, MD, USA), and has been described [7]. U2OS cells were cultured in Dulbecco's Modified Eagle's Medium (DMEM, Invitrogen, Carlsbad, CA, USA) supplemented with 20% fetal bovine serum (Invitrogen).

Plasmids transfection

MiR-506-expressing and antisense (as) plasmids were prepared with general method. Transfection was performed with Lipofectamine 2000 reagent (Invitrogen), according to the instructions of the manufacturer. The cells that were transfected with plasmid expressing a scrambled sequence were used as control (scr). Transfected cells expressing miR-506, or as-miR-506, or control scr were purified by flow cytometry based on GFP.

Western blot

The protein was extracted from the OS or paired non-tumor tissue from the same patient, or from cultured cells, in RIPA lysis buffer (1% NP40, 0.1% SDS, 100 µg/ml phenylmethylsulfonyl fluoride, 0.5% sodium deoxycholate, in PBS) on ice. The supernatants were collected after centrifugation at 12000× g at 4°C for 20 min. Protein concentration was determined using a BCA protein assay kit (Bio-rad, China), and whole lysates were mixed with 4×SDS load-

ing buffer (125 mmol/l Tris-HCl, 4% SDS, 20% glycerol, 100 mmol/l DTT, and 0.2% bromophenol blue) at a ratio of 1:3. Samples were heated at 100°C for 5 min and were separated on SDS-polyacrylamide gels. The separated proteins were then transferred to a PVDF membrane. The membrane blots were first probed with a primary antibody. After incubation with horseradish peroxidase-conjugated second antibody, autoradiograms were prepared using the enhanced chemiluminescent system to visualize the protein antigen. The signals were recorded using X-ray film. Primary antibodies were rabbit anti-Snail2 and anti-α-tubulin (Cell Signaling, San Jose, CA, USA). Secondary antibody is HRP-conjugated anti-rabbit (Jackson Immuno Research Labs, West Grove, PA, USA). Blotting images were representative from 5 repeats. α-tubulin was used as a protein loading control.

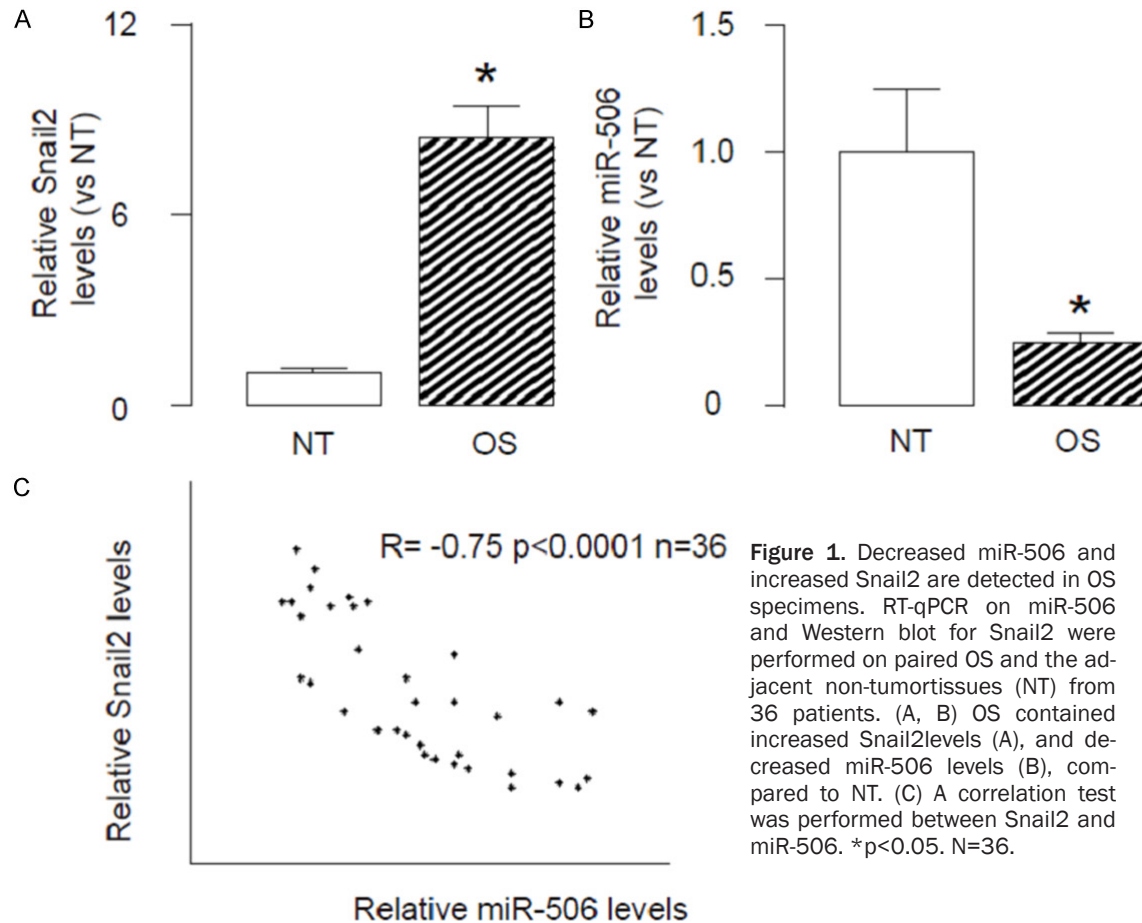
RT-qPCR

Total RNA was extracted from resected specimens from the patients or from cultured cells with miRNeasy mini kit (Qiagen, Hilden, Germany) for cDNA synthesis. Complementary DNA (cDNA) was randomly primed from 2 µg of total RNA using the Omniscript reverse transcription kit (Qiagen). Real-time quantitative PCR (RT-qPCR) was subsequently performed in triplicate with a 1:4 dilution of cDNA using the QuantitectSyBr green PCR system (Qiagen). Quantitative PCR (RT-qPCR) were performed in duplicates with QuantiTect SYBR Green PCR Kit (Qiagen). All primers were purchased from Qiagen. Data were collected and analyzed using 2-ΔΔCt method for quantification of the relative mRNA expression levels. Values of genes were first normalized against α-tubulin, and then compared to controls.

Luciferase-reporter activity assay

Luciferase-reporters were successfully constructed using molecular cloning technology. Target sequence for Snail2 miRNA 3'-UTR clone was purchased from Creative Biogene (Shirley, NY, USA). MiR-506-modified U2OS cells were seeded in 24-well plates for 24 hours, after which the cells were transfected with 1 µg of Luciferase-reporter plasmids per well. Luciferase activities were measured using the dual-luciferase reporter gene assay kit (Promega, Beijing, China), according to the manufacturer's instructions.

MiR-506 inhibits Snail2-mediated metastasis of OS



Transwell cell invasion assay

Cells (10^4) were plated into the top side of polycarbonate transwell filter coated with Matrigel in the upper chamber of the BioCoat™ Invasion Chambers (Becton-Dickinson Biosciences, Bedford, MA, USA) and incubated at 37°C for 22 hours. The cells inside the upper chamber with cotton swabs were then removed. Migratory and invasive cells on the lower membrane surface were fixed, stained with hematoxylin, and counted for 10 random 100X fields per well. Cell counts are expressed as the mean number of cells per field of view. Five independent experiments were performed and the data are presented as mean \pm standard deviation (SD).

Scratch wound healing assay

Scratch wound healing assay was performed as has been described previously [28]. Cells were seeded in 24-well plates at a density of

10^4 cells/well in complete DMEM and cultured to confluence. The cell monolayer was serum starved overnight in DMEM prior to initiating of the experiment. Confluent cell monolayer were then scraped with a yellow pipette tip to generate scratch wounds and washed twice with media to remove cell debris. Cells were incubated at 37°C for 24 hours. Time lapse images were captured after 12 hours using a Nikon Eclipse TE2000-5 microscope. Images were captured from five randomly selected fields in each sample, and the wound areas are calculated by NIH ImageJ software (Bethesda, MA, USA).

Statistical analysis

All statistical analyses were carried out using the SPSS 17.0 statistical software package. Bivariate correlations were calculated by Spearman's Rank Correlation Coefficients. All values were depicted as mean \pm standard deviation and were considered significant if $p <$

MiR-506 inhibits Snail2-mediated metastasis of OS

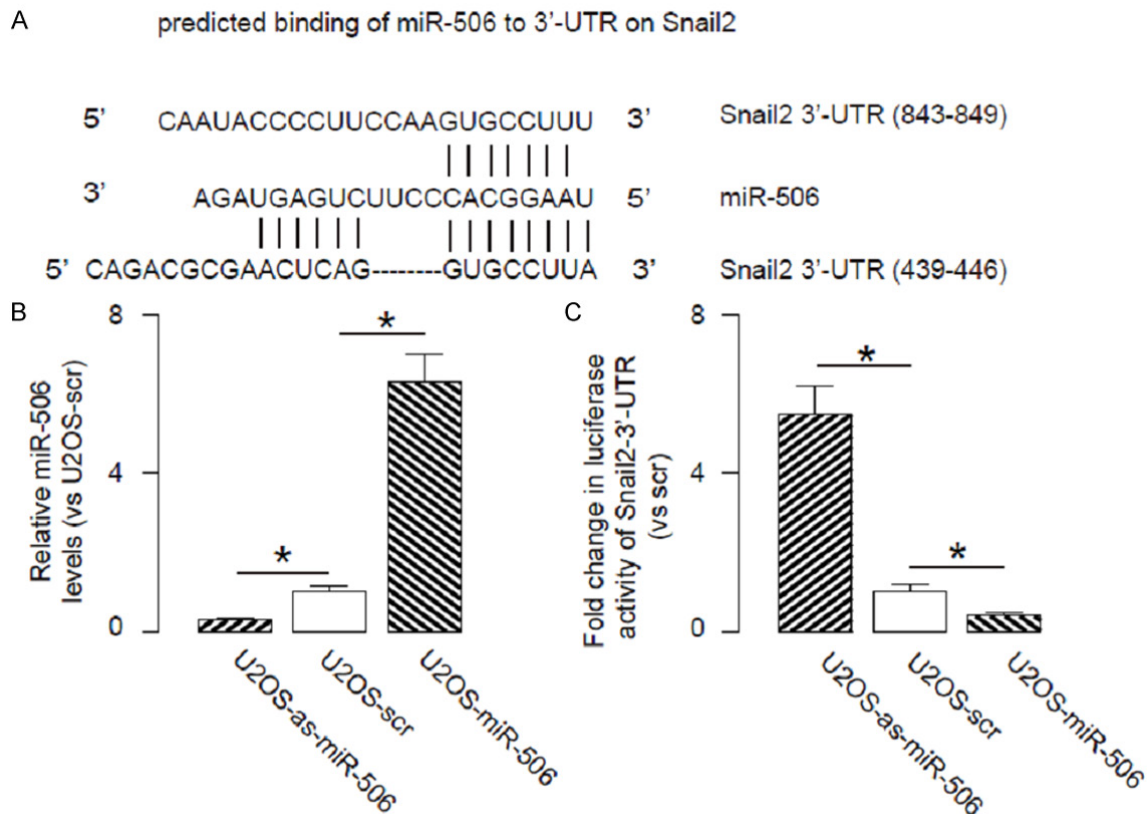


Figure 2. MiR-506 targets 3'-UTR of Snail2 mRNA to inhibit its translation. A. Bioinformatics analyses of binding of miR-506 to the 3'-UTR of Snail2 mRNA. B. In order to examine whether miR-506 may regulate Snail2 in OS cells, we used a human OS cell line, U2OS. We either overexpressed miR-506, or inhibited miR-506 in U2OS cells by transfection of the cells with a miR-506-expressing plasmid (U2OS-miR-506), or with a plasmid carrying miR-506 antisense (U2OS-as-miR-506). The U2OS cells were also transfected with a plasmid carrying a scrambled sequence as a control (U2OS-scr). The overexpression or inhibition of miR-506 in U2OS cells was confirmed by RT-qPCR. C. MiR-506-modified U2OS cells were then transfected with 1 μ g of Snail2-3'UTR luciferase-reporter plasmid. The luciferase activities were quantified in these cells. * $p < 0.05$. N=5.

0.05. All data were statistically analyzed using one-way ANOVA with a Bonferroni correction, followed by Fisher's Exact Test for comparison of two groups.

Results

Decreased miR-506 and increased Snail2 are detected in OS specimens

In the OS samples, we detected significantly higher levels of Snail2 (**Figure 1A**). In order to figure out how miRNAs may be involved in the carcinogenesis of OS, we screened miRNAs in the OS specimens. Among these miRNAs, we detected significantly lower levels of miR-506 in OS, compared to the adjacent non-tumor tissue (NT) from the same patient (**Figure 1B**).

Inverse correlation is detected between miR-506 and Snail2 in OS specimens

To figure out the relationship between miR-506 and Snail2 in OS, we examined the 360S specimen. A strong inverse correlation between miR-506 and Snail2 was detected (**Figure 1C**, $\gamma = -0.75$, $p < 0.0001$). These data suggest the presence of a relationship between miR-506 and Snail2 in OS.

MiR-506 targets 3'-UTR of Snail2 mRNA to inhibit its expression

Since our data suggest a relationship between miR-506 and Snail2 in OS cells, we checked whether miR-506 may target Snail2 mRNA. Our data show that the miR-506 binding sites in the Snail2 mRNA sequence 3'-UTR ranged from

MiR-506 inhibits Snail2-mediated metastasis of OS

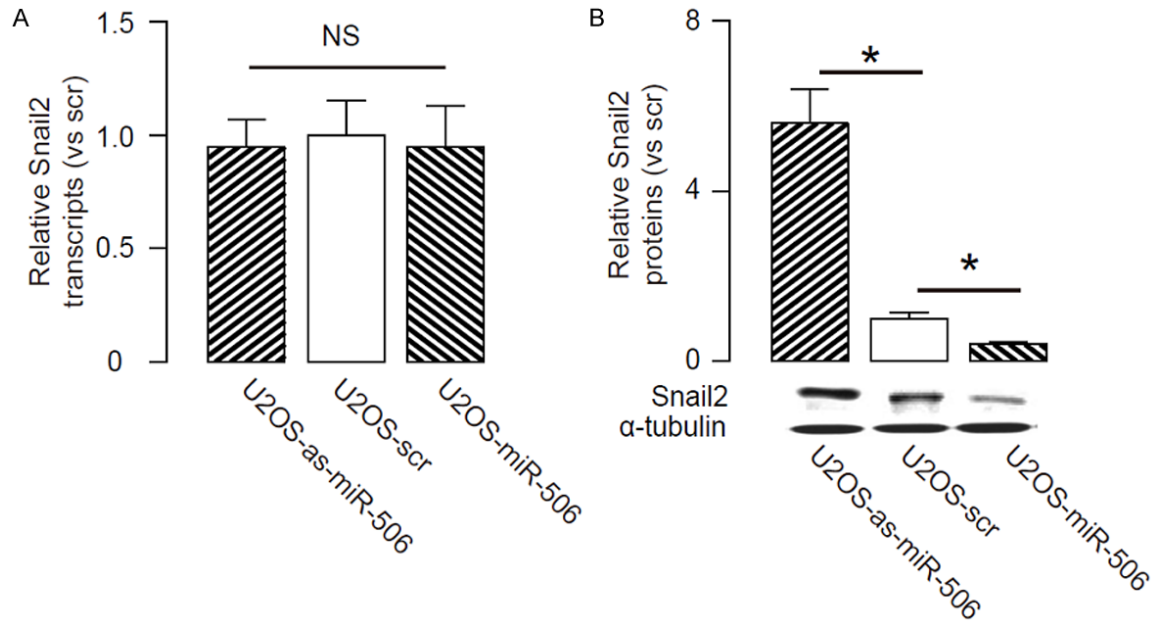


Figure 3. MiR-506 inhibits Snail2 in OS cells. (A, B) RT-qPCR (A) and Western blot (B) for Snail2 in miR-506-modified U2OS cells. * $p < 0.05$. NS: non-significant. N=5.

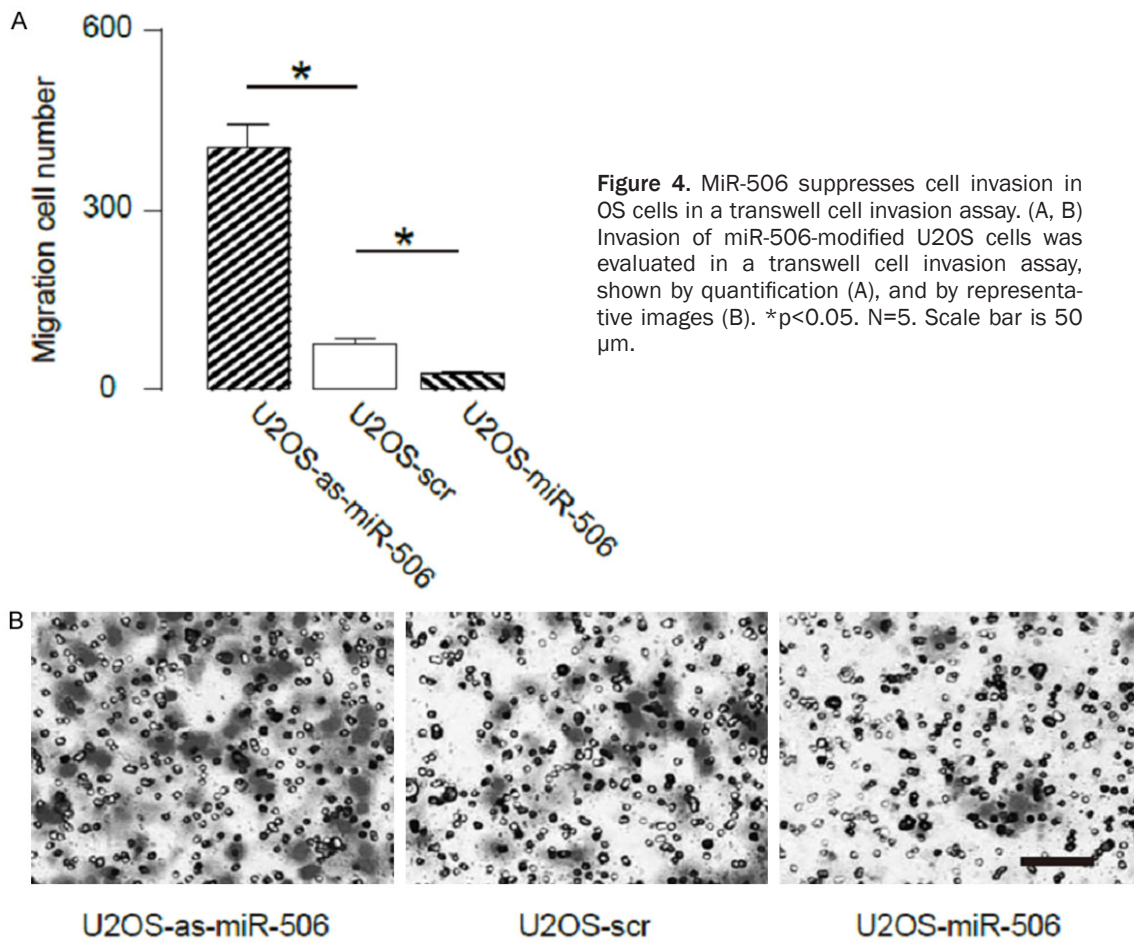


Figure 4. MiR-506 suppresses cell invasion in OS cells in a transwell cell invasion assay. (A, B) Invasion of miR-506-modified U2OS cells was evaluated in a transwell cell invasion assay, shown by quantification (A), and by representative images (B). * $p < 0.05$. N=5. Scale bar is 50 μm .

MiR-506 inhibits Snail2-mediated metastasis of OS

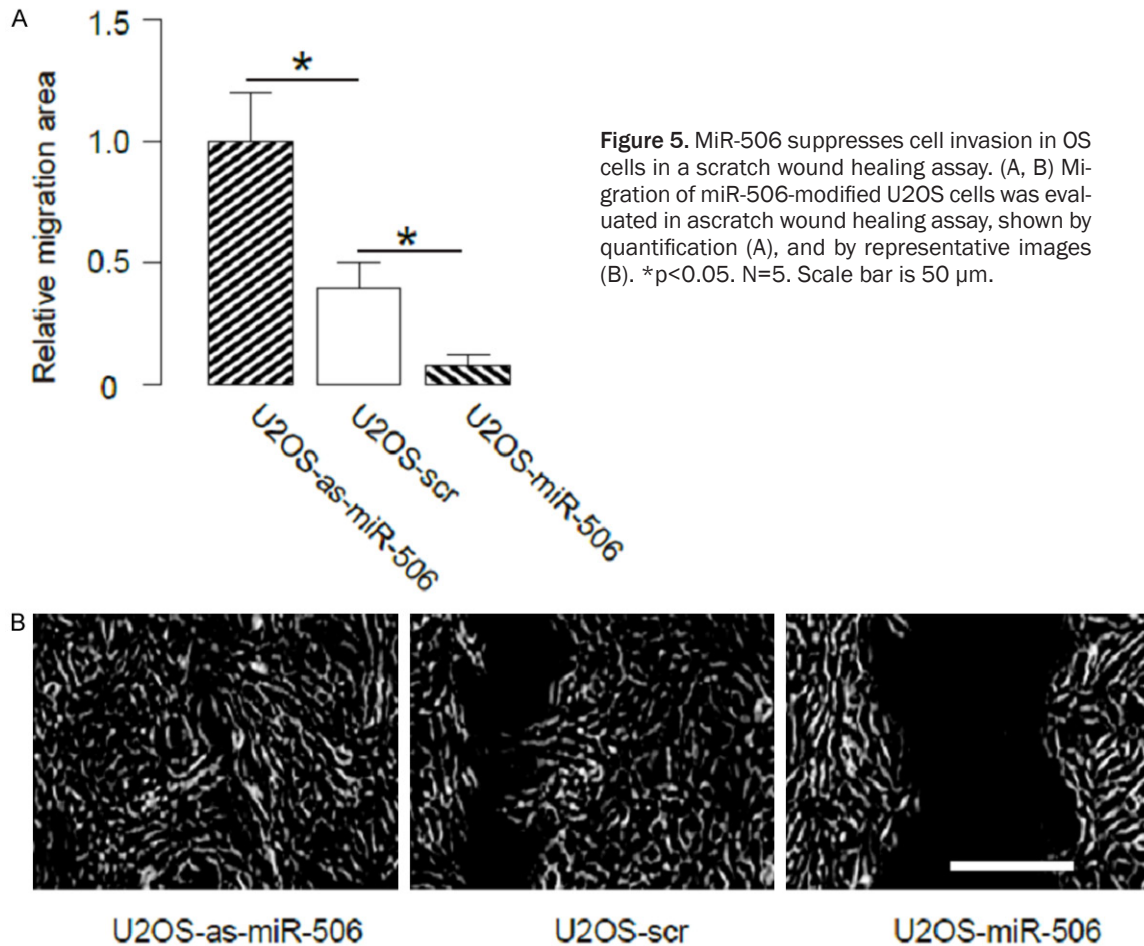


Figure 5. MiR-506 suppresses cell invasion in OS cells in a scratch wound healing assay. (A, B) Migration of miR-506-modified U2OS cells was evaluated in a scratch wound healing assay, shown by quantification (A), and by representative images (B). * $p < 0.05$. N=5. Scale bar is 50 μm .

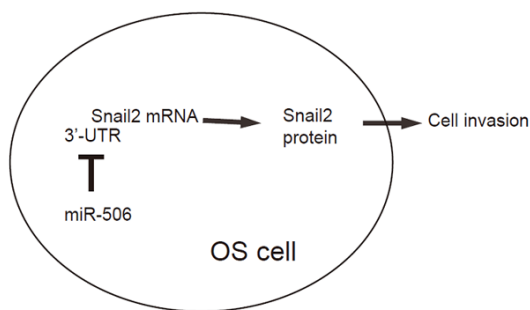


Figure 6. Schematic of the model. MiR-506 inhibits OS cell invasion through Snail2 suppression.

439th base site to 446th base site, and from 843th base site to 849th base site (**Figure 2A**).

In order to examine whether miR-506 may regulate Snail2 in OS, we used a human OS cell line, U2OS. We either overexpressed miR-506, or inhibited miR-506 in U2OS cells by transfection of the cells with a miR-506-expressing plasmid

(U2OS-miR-506), or with a plasmid carrying miR-506 antisense (U2OS-as-miR-506). The U2OS cells were also transfected with a plasmid carrying a scrambled sequence as a control (U2OS-scr). Co-expression of a GFP reporter in these plasmids allow purification of transfected cells by flow cytometry. The overexpression or inhibition of miR-506 in U2OS cells was confirmed by RT-qPCR (**Figure 2B**).

MiR-506-modified U2OS cells were then transfected with 1 μg of Snail2-3'-UTR luciferase-reporter plasmid. The luciferase activities were quantified in these cells, suggesting that miR-506 targets 3'-UTR of Snail2 mRNA to inhibit its translation (**Figure 2C**).

MiR-506 inhibits Snail2 in OS cells

We found that alteration of miR-506 in U2OS cells did not change mRNA of Snail2 (**Figure 3A**). However, overexpression of miR-506 significantly decreased Snail2 protein levels in

MiR-506 inhibits Snail2-mediated metastasis of OS

U2OS cells, while inhibition of miR-506 significantly increased Snail2 protein levels in U2OS cells, by Western blot (**Figure 3B**). These data suggest that MiR-506 inhibits Snail2 protein translation in U2OS cells.

MiR-506 suppresses cell invasion in GC cells

We found that overexpression of miR-506 resulted in decreases in cell invasion of U2OS cells in a transwell cell invasion assay, shown by quantification (**Figure 4A**), and by representative images (**Figure 4B**). Similarly, depletion of miR-506 resulted in increases in cell invasiveness of U2OS cells, shown by quantification (**Figure 4A**), and by representative images (**Figure 4B**). Moreover, we found that overexpression of miR-506 resulted in decreases in cell invasiveness of U2OS cells in a scratch wound healing assay, shown by quantification (**Figure 5A**), and by representative images (**Figure 5B**). Similarly, depletion of miR-506 resulted in increases in cell invasiveness of U2OS cells in a Scratch wound healing assay, shown by quantification (**Figure 5A**), and by representative images (**Figure 5B**). Together, these data suggest that miR-506 inhibits OS cell invasion through Snail2 suppression (**Figure 6**).

Discussion

Many miRNAs play important roles in the invasion and metastasis of OS cells. Therefore, understanding of the aberrant expression of miRNAs in OS cells may help to clarify the mechanisms underlying OS metastasis and thus to improve therapy.

By sequence matching, we found a number of candidate miRNAs that target Snail2, including miR-1, miR-203, miR-30, miR-384-5p, miR-124, miR-506, miR-206, miR-613, etc. Among all these miRNAs, we specifically detected a significant decrease in miR-506 in OS specimen, compared to the paired normal bone tissue. Hence, we hypothesize that miR-506 may target and regulate Snail2 in OS cells. Correlation test further supports this hypothesis in that the levels of miR-506 in GC tissues were inversely correlated with the levels of Snail2 in GC patients. These data suggests that miR-506 may bind Snail2 mRNA to impair its translation.

Overexpression of miR-506 inhibited cell invasion, while depletion of miR-133 increased cell

invasion. Moreover, in miR-506-modified OS cells, we found that the alteration in miR-506 levels did not affect Snail2 mRNA, but regulated the protein level. By promoter luciferase assay, we concluded that miR-506 inhibited Snail2 through translation suppression. Moreover, miR-506-suppressed Snail2 levels resulted in changes in cell invasiveness.

We have examined several other OS cell lines and got essentially similar results. Thus, a possibility of the results to be cell-line-dependence could be excluded. To summarize, we propose a model that regulates OS metastases. Snail2 promotes cell invasion. MiR-506 suppresses Snail2 protein translation, and subsequently decreases cell metastasis. Thus, our study highlights miR-506 as a promising novel target for OS therapy.

Disclosure of conflict of interest

None.

Address correspondence to: Zhongxiang Yu, Department of Orthopaedics, Shu Guang Hospital Affiliated to Shanghai Traditional Chinese Medical University, 528 Zhangheng Road, Pudong New Area, Shanghai 201203, China. Tel: +862120256366; Fax: +862120256366; E-mail: zhongxiang_yu15@163.com

References

- [1] Tsuchiya H, Tomita K, Mori Y, Asada N, Morinaga T, Kitano S and Yamamoto N. Caffeine-assisted chemotherapy and minimized tumor excision for nonmetastatic osteosarcoma. *Anticancer Res* 1998; 18: 657-666.
- [2] Yang J and Zhang W. New molecular insights into osteosarcoma targeted therapy. *Curr Opin Oncol* 2013; 25: 398-406.
- [3] Li G, Fu D, Liang W, Fan L, Chen K, Shan L, Hu S, Ma X, Zhou K and Cheng B. CYC1 silencing sensitizes osteosarcoma cells to TRAIL-induced apoptosis. *Cell Physiol Biochem* 2014; 34: 2070-2080.
- [4] Liu Y, He J, Chen X, Li J, Shen M, Yu W, Yang Y and Xiao Z. The proapoptotic effect of formononetin in human osteosarcoma cells: involvement of inactivation of ERK and Akt pathways. *Cell Physiol Biochem* 2014; 34: 637-645.
- [5] Wang Q, Cai J, Wang J, Xiong C and Zhao J. MiR-143 inhibits EGFR-signaling-dependent osteosarcoma invasion. *Tumour Biol* 2014; 35: 12743-12748.

MiR-506 inhibits Snail2-mediated metastasis of OS

- [6] Xiao Q, Zhang X, Wu Y and Yang Y. Inhibition of macrophage polarization prohibits growth of human osteosarcoma. *Tumour Biol* 2014; 35: 7611-7616.
- [7] Ponten J and Saksela E. Two established in vitro cell lines from human mesenchymal tumours. *Int J Cancer* 1967; 2: 434-447.
- [8] Li W, Jiang G, Zhou J, Wang H, Gong Z, Zhang Z, Min K, Zhu H and Tan Y. Down-regulation of miR-140 induces EMT and promotes invasion by targeting Slug in esophageal cancer. *Cell Physiol Biochem* 2014; 34: 1466-1476.
- [9] Qiu YH, Wei YP, Shen NJ, Wang ZC, Kan T, Yu WL, Yi B and Zhang YJ. miR-204 inhibits epithelial to mesenchymal transition by targeting slug in intrahepatic cholangiocarcinoma cells. *Cell Physiol Biochem* 2013; 32: 1331-1341.
- [10] Niu H, Wu B, Jiang H, Li H, Zhang Y, Peng Y and He P. Mechanisms of RhoGDI2 mediated lung cancer epithelial-mesenchymal transition suppression. *Cell Physiol Biochem* 2014; 34: 2007-2016.
- [11] Deng X, Wu B, Xiao K, Kang J, Xie J, Zhang X and Fan Y. MiR-146b-5p promotes metastasis and induces epithelial-mesenchymal transition in thyroid cancer by targeting ZNRF3. *Cell Physiol Biochem* 2015; 35: 71-82.
- [12] Guo J, Xia N, Yang L, Zhou S, Zhang Q, Qiao Y and Liu Z. GSK-3beta and vitamin D receptor are involved in beta-catenin and snail signaling in high glucose-induced epithelial-mesenchymal transition of mouse podocytes. *Cell Physiol Biochem* 2014; 33: 1087-1096.
- [13] Teng Y, Zhao L, Zhang Y, Chen W and Li X. Id-1, a protein repressed by miR-29b, facilitates the TGFbeta1-induced epithelial-mesenchymal transition in human ovarian cancer cells. *Cell Physiol Biochem* 2014; 33: 717-730.
- [14] Yang T, Chen M and Sun T. Simvastatin attenuates TGF-beta1-induced epithelial-mesenchymal transition in human alveolar epithelial cells. *Cell Physiol Biochem* 2013; 31: 863-874.
- [15] Di Leva G and Croce CM. miRNA profiling of cancer. *Curr Opin Genet Dev* 2013; 23: 3-11.
- [16] Pereira DM, Rodrigues PM, Borralho PM and Rodrigues CM. Delivering the promise of miRNA cancer therapeutics. *Drug Discov Today* 2013; 18: 282-289.
- [17] Mei Q, Li F, Quan H, Liu Y and Xu H. Busulfan inhibits growth of human osteosarcoma through miR-200 family microRNAs in vitro and in vivo. *Cancer Sci* 2014; 105: 755-762.
- [18] Wang F, Xiao W, Sun J, Han D and Zhu Y. MiRNA-181c inhibits EGFR-signaling-dependent MMP9 activation via suppressing Akt phosphorylation in glioblastoma. *Tumour Biol* 2014; 35: 8653-8658.
- [19] Liu G, Jiang C, Li D, Wang R and Wang W. MiRNA-34a inhibits EGFR-signaling-dependent MMP7 activation in gastric cancer. *Tumour Biol* 2014; 35: 9801-9806.
- [20] Yu F, Lv M, Li D, Cai H, Ma L, Luo Q, Yuan X and Lv Z. MiR-506 Over-Expression Inhibits Proliferation and Metastasis of Breast Cancer Cells. *Med Sci Monit* 2015; 21: 1687-1692.
- [21] Zhang Z, Ma J, Luan G, Kang L, Su Y, He Y and Luan F. MiR-506 suppresses tumor proliferation and invasion by targeting FOXQ1 in nasopharyngeal carcinoma. *PLoS One* 2015; 10: e0122851.
- [22] Yang FQ, Zhang HM, Chen SJ, Yan Y and Zheng JH. MiR-506 is down-regulated in clear cell renal cell carcinoma and inhibits cell growth and metastasis via targeting FLOT1. *PLoS One* 2015; 10: e0120258.
- [23] Sun Y, Hu L, Zheng H, Bagnoli M, Guo Y, Rupaimoole R, Rodriguez-Aguayo C, Lopez-Berestein G, Ji P, Chen K, Sood AK, Mezzanatica D, Liu J, Sun B and Zhang W. MiR-506 inhibits multiple targets in the epithelial-to-mesenchymal transition network and is associated with good prognosis in epithelial ovarian cancer. *J Pathol* 2015; 235: 25-36.
- [24] Wang Y, Cui M, Sun BD, Liu FB, Zhang XD and Ye LH. MiR-506 suppresses proliferation of hepatoma cells through targeting YAP mRNA 3'UTR. *Acta Pharmacol Sin* 2014; 35: 1207-1214.
- [25] Wu J, Peng X, Zhou A, Qiao M, Wu H, Xiao H, Liu G, Zheng X, Zhang S and Mei S. MiR-506 inhibits PRRSV replication in MARC-145 cells via CD151. *Mol Cell Biochem* 2014; 394: 275-281.
- [26] Wen SY, Lin Y, Yu YQ, Cao SJ, Zhang R, Yang XM, Li J, Zhang YL, Wang YH, Ma MZ, Sun WW, Lou XL, Wang JH, Teng YC and Zhang ZG. miR-506 acts as a tumor suppressor by directly targeting the hedgehog pathway transcription factor Gli3 in human cervical cancer. *Oncogene* 2015; 34: 717-725.
- [27] Liu G, Sun Y, Ji P, Li X, Cogdell D, Yang D, Parker Kerrigan BC, Shmulevich I, Chen K, Sood AK, Xue F and Zhang W. MiR-506 suppresses proliferation and induces senescence by directly targeting the CDK4/6-FOXM1 axis in ovarian cancer. *J Pathol* 2014; 233: 308-318.
- [28] Liang CC, Park AY and Guan JL. In vitro scratch assay: a convenient and inexpensive method for analysis of cell migration in vitro. *Nat Protoc* 2007; 2: 329-333.